Title Page

Detection and Measurement of Rheumatoid Bone and Joint Lesions of Fingers by Tomosynthesis: A Phantom Study for Reconstruction Filter Setting Optimization

Yohei Ono, RT
Graduate School of Health Sciences, Hokkaido University, North-12 West-5, Kita-ku, Sapporo City, 060 0812 Japan.

Tamotsu Kamishima, MD, PhD
Faculty of Health Sciences, Hokkaido University, North-12 West-5, Kita-ku, Sapporo City, 060 0812 Japan.

Nobutoshi Yasojima, RT
Department of Radiology, NTT East Japan Sapporo Hospital, South-1, West-15, Cyuo-ku, Sapporo City, 060 0061 Japan .

Kenichi Tamura, PhD
Department of Mechanical Engineering, College of Engineering, Nihon University, Nakagawara, Tokusada, Tamuramachi, Koriyama, Fukushima Prefecture, 963 8642 Japan.

Kaori Tsutsumi, RT, PhD
Faculty of Health Sciences, Hokkaido University, North-12 West-5, Kita-ku, Sapporo City, 060 0812 Japan.

Address correspondence to:
Tamotsu Kamishima, MD, PhD,
Faculty of Health Sciences, Hokkaido University
North-12 West-5, Kita-ku, Sapporo City, 060 0812 Japan.
Phone/FAX; 81-11-706-2824
E-mail: ktamotamo2@yahoo.co.jp

Detection and Measurement of Rheumatoid Bone and Joint Lesions of Fingers by Tomosynthesis: A Phantom Study for Reconstruction Filter Setting Optimization

Abstract

Rheumatoid arthritis (RA) is a systemic disease that is caused by autoimmunity. RA causes synovial proliferation, which may result in bone erosion and joint space narrowing in the affected joint. Tomosynthesis is a promising modality which may detect early bone lesions such as small bone erosion and slight joint space narrowing. Nevertheless, so far, the optimal reconstruction filter for detection of early bone lesions of fingers on tomosynthesis has not yet been known. Our purpose in this study was to determine an optimal reconstruction filter setting by using a bone phantom. We obtained images of a cylindrical phantom with holes simulating bone erosions (diameters of 0.6, 0.8, 1.0, 1.2, and 1.4 mm) and joint spaces by aligning two phantoms (space widths from 0.5 mm to 5.0 mm with 0.5 mm intervals), examining 6 reconstruction filters by using tomosynthesis. We carried out an accuracy test of the bone erosion size and joint space width, done by one radiological technologist, and a test to assess the visibility of bone erosion, done by 5 radiological technologists. No statistically significant difference was observed in the measured bone erosion size and joint space width among all of the reconstruction filters. In the visibility assessment test, reconstruction filters of Thickness+- and Thickness-- were among the best statistically in all characteristics except the signal to noise ratio. The Thickness+- and Thickness-- reconstruction filter may be optimal for evaluation of RA bone lesions of small joints in tomosynthesis.

Key Words

tomosynthesis, bone erosion, joint space narrowing, bone phantom, reconstruction filter

Introduction

Rheumatoid arthritis (RA) is a common systemic disease caused by autoimmunity. Synovial proliferation is the hallmark of RA, which may lead to RA bone lesions, such as bone erosion and joint space narrowing around bones of the affected joint [1,2]. The joint destruction arising from RA bone lesions causes significant functional impairment, with a consequent reduction in quality of life (QOL) [3]. The diagnosis of RA is traditionally based on radiographic findings. Radiography is also used for the staging and follow-up in patients with RA and for assessment of treatment effectiveness [4]. However, radiography has disadvantages such as a low sensitivity for detection of early RA bone lesions because the three-dimensional joint structure is projected onto a two-dimensional image, whereas it has advantages such as a short examination time and low cost. Computed tomography (CT) has a high detection ability, but the exposure dose is much higher than that for radiography [5, 6].

Tomosynthesis indicates an arbitrary section of a three-dimensional image by collecting a number of projected images at different angles with a digital detector [7]. Therefore, tomosynthesis can detect overlapping structures clearly, whereas it may be difficult to evaluate them by radiography [8, 9]. For that reason, tomosynthesis is expected to detect more early RA bone lesions than does radiography. In addition, the

exposure dose in tomosynthesis is only a little higher than that in radiography while it maintains sufficient diagnostic information [10]. For example, in an investigation by Aoki, et al., the mean total radiation dose of radiography and tomosynthesis for the wrist and hand was 0.13 mGy and 0.25 mGy, respectively [11]. Tomosynthesis has advantages regarding detection ability and exposure dose, but the optimal imaging setting for detecting RA bone lesions by tomosynthesis has not been fully established.

Among imaging parameter settings for tomosynthesis, the sweep angle and sweep direction have already been investigated; however, the selection of an optimal reconstruction filter remains unknown [12]. In this study, we determined an optimal reconstruction filter to observe RA bone lesions among 6 reconstruction filters installed in a tomosynthesis instrument made by SHIMADZU, Kyoto, Japan. According to the technical description issued by SHIMADZU, the reconstruction filter affects the degree of frequency band limitation, which affects the reconstruction slice thickness and the artifacts on the reconstruction image. The reconstruction slice thickness and artifacts on the reconstruction image may influence the evaluation of RA bone lesions, because it is visually performed by a rheumatologist or radiologist [13, 14]. The progression of joint destruction is fast at the early stage of RA, however, it is difficult to detect and evaluate early bone lesions on radiologic images [15, 16]. Accurate detection and evaluation of

early bone lesions are linked to an immediate initiation of treatment and the determination of appropriate treatment strategy, which leads to the suppression of reduction in QOL as much as possible. Therefore, the determination of a reconstruction filter with which the RA bone lesion detection ability is higher could be crucial.

Additionally, it is necessary to reproduce an accurate bone erosion size and joint space width, because it is one of the indices for determining an optimal reconstruction filter. We used a phantom made of titanium medical apatite (TMA) [17], which has an X-ray absorption similar to that of bone, with plasticity for processing of details such as tiny bone erosion.

Therefore, our purpose in our phantom study was the determination of an optimal reconstruction filter for detection of RA bone lesions in the finger by tomosynthesis.

Materials and methods

Setups and preparation of phantom with bone erosion

This study was performed with a commercially available tomosynthesis instrument (SONIALVISION safire Ⅱ; SHIMADZU, Kyoto, Japan). We prepared a cylindrical phantom with 5 dents of different sizes simulating bone erosion, with diameters of 0.6, 0.8 1.0, 1.2, and 1.4 mm (Fig 1). The phantom was made of TMA. TMA is a recently

introduced material that has easier processing than does hydroxyapatite, and its CT value (Hounsfield unit) is nearly equal to that of bone [17]. The diameter and length of the phantom were 11 mm and 35 mm, respectively.

Accuracy assessment of bone erosion size

We obtained 6 image series in the coronal and sagittal planes that had different characteristics by using 6 reconstruction filters: Thickness++, Thickness++(Metal2), Thickness+-, Thickness+-(DC2), Thickness--, and Thickness--(Contrast2). According to a technical description published by SHIMADZU, the degree of frequency band limitation for reduction of artifacts is different for each reconstruction filter. Reconstruction filters of the Thickness++ system, Thickness+- system, and Thickness-- system have high, medium, and low band limitation, respectively. Thickness++(Metal2), Thickness+-(DC2), and Thickness--(Contrast2) are modified versions of Thickness++, Thickness+-, and Thickness-- system, respectively. Here, DC of Thickness+-(DC2) means direct current.

We obtained images by using imaging parameter for routine hand study for RA patients (Table 1). Each bone erosion size on reconstruction images was measured by image analysis software, ImageJ (National Institutes of Health, Bethesda, MD, USA,

http://rsbweb.nih.gov/ij/) on the basis of full width at half maximum of the bone erosion signal in the profile curve (Fig 2). The errors in the measurement of bone erosion size by tomosynthesis were calculated and compared among the reconstruction filters. In this study, the measured value of bone erosion size in the CT image was used as the gold standard of bone erosion size in the reconstruction image because CT is superior to tomosynthesis for accurate detection of bone erosion [8].

$$Error = |\ Measured\ value\ using\ CT - Measured\ value\ using\ tomosynthesis\ |$$

Visibility assessment test

Receiver operating characteristic (ROC) analysis was performed as a visibility assessment test. The monitor used in this test was Flex Scan EV2335W (EIZO NANAO Corporation, Ishikawa, Japan), whose maximum resolution was 1920 × 1080. The readers were 5 radiological technologists (work experience less than one year). The samples for ROC analysis were made in the size of 512×512 pixels to include 0 or 1 bone erosion in reconstruction images. Image segmentation was performed to prevent the readers from judging the presence or absence of bone erosion in samples based on the positional relationship between other bone erosions and the location in the phantom

(Fig 3). Twenty-five positive images and 20 negative images for bone erosion were prepared in each reconstruction filter. We varied the reading order of samples in each reader in order to eliminate the bias caused by the reading order. The readers were asked to perform a 5-stage confidence-rating test as follows: 1. bone erosion definitely not present, 2. bone erosion probably not present, 3. unsure, 4. bone erosion probably present, 5. bone erosion definitely present. The five readers evaluated the images; image reading sessions for the next reconstruction image series were started only after the current one was completed. The area under the ROC curve (Az value) of each reconstruction filter were calculated and compared. After definition of positive (4 or 5 points) and negative (1 or 2 points) in the confidence-rating test, the sensitivity, specificity, and accuracy of each reconstruction filter were calculated and compared. Additionally, we created the ROC curve for each reader and calculated the Az value, sensitivity, specificity, and accuracy for each bone erosion size.

Next, we calculated the signal-to-noise ratio (SNR) and contrast in bone erosion images in order to evaluate the characteristic of each reconstruction filter image quantitatively. The SNR and contrast were defined as follows.

$$SNR = N_E / \sigma_B,\ contrast = (N_E - N_B)/N_B$$

N_E is the average pixel value in the simulated bone erosion region of interest (ROI). σ_B

and N_B are the standard deviation and the average pixel value of the background ROI, respectively. These values were measured in black and white inverted images by use of ImageJ. The simulating bone erosion ROI was a square (5 × 5 pixels), and the background ROI was a rectangle (8 × 16 pixels) (Fig 4). The average pixel value in the simulated bone erosions of the tomosynthesis images for each reconstruction filter was measured setting a ROI in those with diameters of 1.4 mm.

Accuracy assessment of joint space narrowing

The tomosynthesis device used in this study was the same as that used in the bone erosion study. Joint space widths from 0.5 mm to 5.0 mm (0.5 mm interval) were made with use of 2 cylindrical phantoms made of TMA (Fig 5). Joint-space widths were set on graph paper, and digital calipers (Plastic Digital Caliper PC-15JN, Mitsutoyo Co. Kawasaki, Japan.) were used for confirmation of the setting. We obtained the images by using a parameter for routine hand study for RA patients (Table 1). The types of reconstruction filters and the method of measurement used in this study were the same as those in the bone erosion study.

Statistical Analysis

All statistical analyses were performed with statistical analysis software, PASW Statistics 18 (SPSS Inc, Chicago, IL, USA). $p < .05$ was considered to indicate a statistically significant difference in all statistical analyses. Analysis of variance with post-hoc Tukey was performed in the accuracy assessment of bone erosion size, which compared the errors between measured values and setting values, and in the visibility assessment test, which compared Az value, sensitivity, specificity, accuracy, SNR, and contrast for each reconstruction filter. The Kruscal-Wallis test was performed in the accuracy assessment of joint space width, which compared the errors between measured values and setting values.

Results

Bone erosion phantom images were obtained in two planes, coronal and sagittal. In bone erosion with a diameter of 0.6 mm, which was the minimum size in this study, it was difficult to discern the noise and bone erosion signal in the profile curve for both imaging planes. Therefore, bone erosion with a diameter of 0.6 mm was eliminated from the analysis, and the accuracy assessment of bone erosion size by image analysis software was performed from a total of 48 bone erosion measurement results, or 8 measurement results (2 planes for each 0.8 1.0, 1.2, and 1.4 mm bone erosion) for 6

reconstruction filter settings. The errors (mean±standard deviation) of bone erosion sizes measured for each reconstruction filter were 0.2660±0.07953 with Thickness++, 0.1962±0.06135 with Thickness++(Metal2), 0.2607±0.06404 with Thickness+-, 0.2660±0.08397 with Thickness+-(DC2), 0.2660±0.1042 with Thickness--, and 0.2309±0.08689 with Thickness--(Contrast2) (Fig 6a). We found that there was some variation in errors, but differences in errors between reconstruction filters were not significant ($p = .509$). Figure 7 shows bone erosion phantom images.

In the visibility assessment test for bone erosion, the difference in Az values was not significant ($p = .072$). On the other hand, significant differences were observed in sensitivity, specificity, accuracy, SNR, and contrast among reconstruction filters ($p = .002$, .007, .002, .000, and .000, respectively). The values for these are shown in Fig 8. Reconstruction filters of Thickness+- and Thickness-- were among the best statistically in all items except the SNR.

In addition, ROC curves for each reader and the 95% confidence interval are shown as supplementary data (Fig S1, Table S1). We found that the Az value for reconstruction filters Thickness++(Metal2) and Thickness+- tended to be low and high, respectively,

whereas there was some variation in the order of the Az values concerning their magnitude among reconstruction filters according to the readers. The error, Az value, sensitivity, specificity, and accuracy for each bone erosion size (diameters of 0.8, 1.0, 1.2, and 1.4 mm) are shown in Fig S2. A negative correlation between bone erosion size and the error was found with Pearson's product-moment correlation coefficient (r = -0.9095). In a similar way, a positive correlation between bone erosion size and Az value, sensitivity, and accuracy was found (r = 0.8845, 0.8971, and 0.8971, respectively).

For accuracy assessment of joint space narrowing, the errors (mean±standard deviation) of joint space width measured for each reconstruction filter were 0.1243±0.06891 with Thickness++, 0.1236±0.06591 with Thickness++(Metal2), 0.1103±0.08800 with Thickness+-, 0.09398±0.07266 with Thickness+-(DC2), 0.1198±0.09941 with Thickness--, and 0.1477±0.08042 with Thickness--(Contrast2) (Fig 6b). The difference in the error of the joint space width was not significant (p = .634). Figure 9 shows joint space phantom images obtained in this study.

Discussion

Detection of early bone erosion and joint space narrowing is crucial for control of the progression of RA and for keeping the QOL of the RA patients by initiating timely treatment [15, 16]. Recently, tomosynthesis has become expected to play a role in early detection of destructive changes of bone in clinical images [8, 11]. However, no information for selection of reconstruction filters was available in previous articles, and a study to determine an optimal reconstruction filter as one of the imaging settings for tomosynthesis has not been performed in the context of detecting early RA bone lesions to the best of our knowledge.

In this study, we assumed that the RA bone lesion detection ability in tomosynthesis is improved by the selection of an appropriate reconstruction filter. We reproduced bone erosion and joint space in reconstruction images of a phantom by using various filters. We determined the filter with which bone lesions can be measured most accurately, and also the filter with the highest visibility for observing bone erosion.

In the accuracy assessment of RA bone lesion measurement in reconstruction images, the measurement accuracy was nearly the same for all of the reconstruction filters which we examined. This result may be explained by the following: the reconstruction filter not only affects artifacts and contrast on reconstruction images, but also the depth resolution, because of the inherent reconstruction slice thickness that is unique to each

reconstruction filter. The depth resolution is affected by the proportion of effective data in frequency space, which depends on the degree of band limitation that is specific to reconstruction filters. In this study, the depth resolution did not affect the measurement results in the reconstruction image. This may be attributed to the shape of the phantom; the joint space width was kept constant regardless the depth of the joint space, and all bone erosions were small and were reproduced only at the surface of the phantom (maximum depth of 0.7 mm).

On the other hand, in the visibility assessment test of bone erosion, significant differences were observed in sensitivity, specificity, accuracy, SNR, and contrast among reconstruction filters, whereas the difference in Az values was not significant ($p = .072$). When we consider that the Az value expresses the "overall accuracy" of the test and there was a statistically significant difference in sensitivity, specificity, and accuracy, an increase in sample size (number of images and/or readers) in ROC analysis should improve the p-value for the Az value. Reconstruction filters of Thickness+- and Thickness-- were among the best statistically in all characteristics except the SNR. When the signal of bone erosion was emphasized against the background in reconstruction images, the readers could easily judge the presence or absence of bone erosion. This is further proved in the assessment of the contrast between bone erosion

and background for each reconstruction filter. The contrast of Thickness+- and Thickness-- was significantly higher than that of the other reconstruction filters.

Specificity was higher than sensitivity in the visibility assessment test. Sensitivity is the percentage that readers considered as positive among positive images, and specificity is the percentage that readers considered as negative among negative images. It was considered that this result was caused by the following. In this study, the difficulty level of the correct judgment for positivity increased because bone erosion with a diameter of 0.6 mm was contained in positive images. In bone erosion with a diameter of 0.6 mm, it was difficult to discern the noise and the bone erosion signal in the profile curve. Additionally, readers found it easy to judge negative images correctly.

Detection of small bone erosions with high accuracy is clinically significant in early RA diagnosis or in follow up of RA patients, which could be directly linked to improvement in the quality of treatment. Thus, selecting reconstruction filters with high visibility for bone erosion detection, such as Thickness+- and Thickness--, might be very important clinically, where there is no need for concern about risk of additional examination time or dose increase to patients. Although the reconstruction filters of Thickness+- and Thickness-- were lower in SNR than those of the Thickness++ group, we believe that these reconstruction filters are optimal and we recommend these in

terms of clinical utility, namely, the accurate detection of RA bone lesions.

We acknowledge that our study has several limitations. First, the data were obtained only from a phantom study. Therefore, we cannot state clearly whether the results of this study can be extrapolated to the clinical situation. However, we took special care so that the bone CT value, bone erosion size, and joint space width in the phantom were almost equivalent to the actual ones. Second, an assessment of implanted metal was not performed in this study, although the 6 reconstruction filters used contained a filter with characteristics that reduced the metal artifact. Third, no tomosynthesis instrument was tested other than SONIALVISION safire Ⅱ (SHIMADZU, Japan) in this study. An additional study with tomosynthesis instruments made by other manufacturers may be necessary for confirmation whether the results obtained in this study are applicable universally.

In conclusion, in this study we determined the reconstruction filter that can most accurately detect RA bone lesions in small joints by tomosynthesis. The reconstruction filters of Thickness+- and Thickness-- whose band limitation is moderate and low were optimized because they had accurate joint width reproduction ability and improved visibility for bone erosion.

Conflict of interest:

The authors declare that they have no conflict of interest.

References

1. Sommer OJ, Kladosek A, Weiler V, et al. Rheumatoid arthritis: a practical guide to state-of-the-art imaging, image interpretation, and clinical implications. Radiographics. 2005 Mar-Apr;25(2):381-98.

2. van der Heijde DM. Joint erosions and patients with early rheumatoid arthritis. Br J Rheumatol. 1995 Nov;34 Suppl 2:74-8.

3. Roma I, Almeida ML, Mansano Nda S, et al. [Quality of life in adults and elderly patients with rheumatoid arthritis]. Rev Bras Rheumatol, 2014 Jun-Aug; 54(4): 279-86

4. van der Heijde DM. Radiographic imaging: the 'gold standard' for assessment of disease progression in rheumatoid arthritis. Rhematology(Oxford). 2000 Jun;39 Suppl 1:9-16.

5. Salaffi F, Darotti M, Ciapetti A, et al. Validity of a computer-assisted manual segmentation software to quantify wrist erosion volume using computed tomography

scans in rheumatoid arthritis, BMC Musculoskelet Disrd, 2013 Sep 12; 14:265

6. Jornada Tda S, da Silva TA. Determination of dosimetric quantities in pediatric abdominal computed tomography scans, Radiol Bras, 2014 Sep-Oct; 47(5):288-91

7. Dobbins JT 3rd, Godfrey DJ. Digital x-ray tomosynthesis: current state of the art and clinical potential. Phys Med Biol. 2003 Oct 7;48(19):R65-109.

8. Canella C, Philippe P, Pansini V, et al. Use of Tomosynthesis for Erosion Evaluation in Rheumatoid Arthritic Hands and Wrists. Radiology. 2011 Jan;258(1) :199-205.

9. Vikgren J, Zachrisson S, Svalkvist A, et al. Comparison of chest tomosynthesis and chest radiography for detection of pulmonary nodules: human observer study of clinical cases. Radiology. 2008;249 :1034–1041.

10. Hwang HS, Chung MJ, Lee KS. Digital tomosynthesis of the chest: comparison of patient exposure dose and image quality between standard default setting and low dose setting. Korean Journal of Radiology. 2013 May-Jun; 14(3):525-531.

11. Aoki T, Fujii M, Yamashita Y, et al. Tomosynthesis of the Wrist and Hand in Patients With Rheumatoid Arthritis: Comparison With Radiography and MRI. AJR Am J Roentgenol. 2014 Feb;202(2):386-90

12. Machida H, Yuhara T, Mori T, et al. Optimizing Parameters for Flat-Panel Detector Digital Tomosynthesis. Radiographics. 2010 Mar;30(2) : 549-62.

13. Tutoğlu A, Boyaci A, Botaci N, et al. Is There Any Relationship between Joint Destruction and Carotid Intima-media Thickness in Patients with Rheumatoid Arthritis? J Phys Ther Sci, 2014 Jul; 26(7): 1093-6

14. van der heijde D. How to read radiographs according to the Sharp/van der Heijde method. J Rheumatol, 2000 Jan; 27(1): 261-315. Fuchs HA, Kaye JJ, Nabce EP, et al. Evidence of significant radiographic damage in rheumatoid arthritis within the first 2 years of disease. J Rheumatol, 1989 May;16(5):585-91.

16. Mottonen TT, Prediction of erosiveness and rate of development of new erosions in

early rheumatoid arthritis. Ann Rheum Dis, 1988 Aug; 47(8): 648-53

17. Tamura K, Fujita T, Morisaki Y. Vacuum-sintered body of a novel apatite for artificial bone. Central European Journal of Engineering. 2013 3(4): 700-706.

Figure

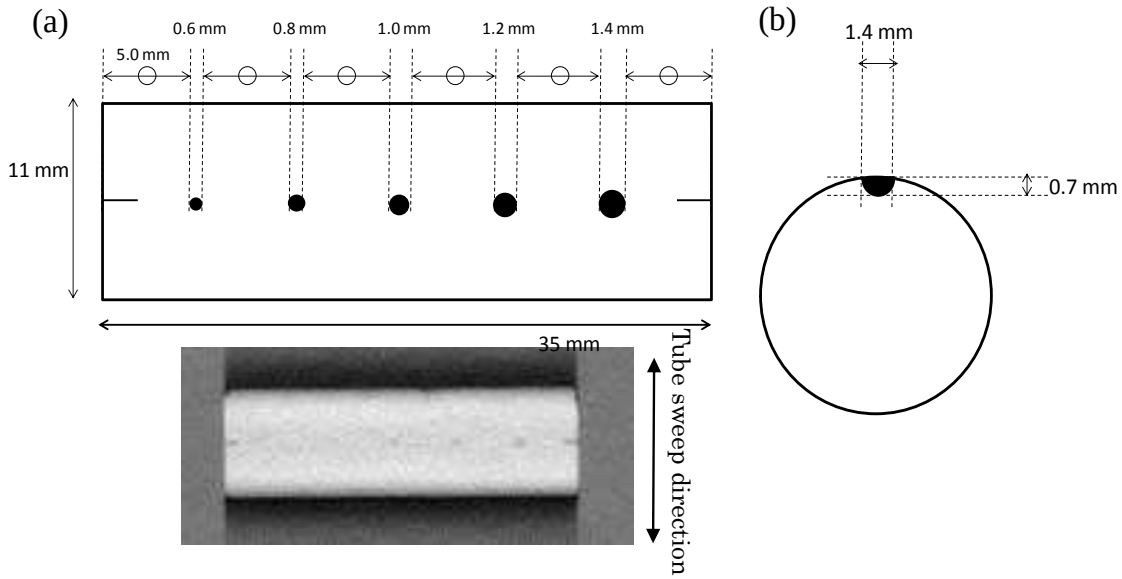

Fig 1 Detailed sizes of bone erosion phantom.

a. Top view. b. Side view

Bone erosion with a diameter of 1.4 mm is demonstrated as an example; the depth of the bone erosion was set at half the size of its diameter.

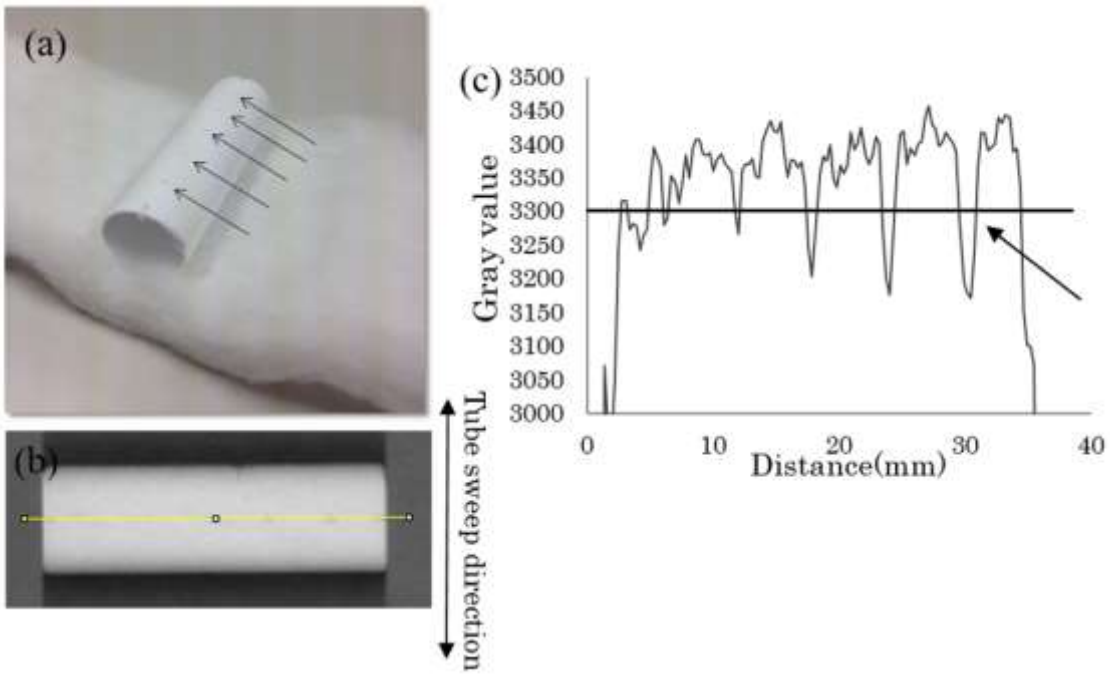

Fig 2 Bone erosion measurement with use of a phantom.

a. Photograph of the cylindrical phantom used in this study. Arrows indicate the locations of bone erosion. b. The part selected to depict profile curve. c. Profile curve of the selected part and linear graph with a gray scale value of around 3300 corresponding to full width at half maximum of the signal for the largest bone erosion sized 1.4 mm (c, arrow).

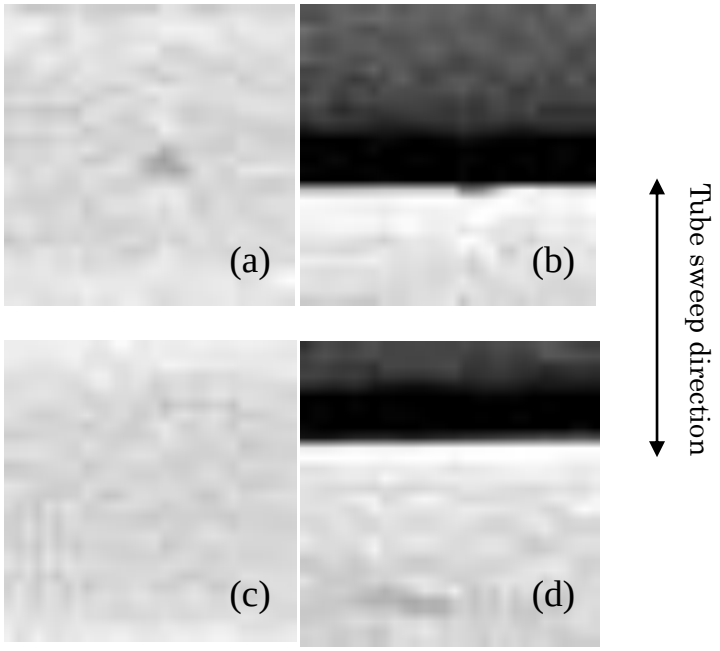

Fig 3 Segmented image samples (positive and negative for bone erosion) in ROC analysis.

a. Positive image (coronal section). b. Positive image (sagittal section). c. Negative image (coronal section). d. Negative image (sagittal section)

Negative images are derived from the region where there is no erosion prepared in the phantom, and they were utilized in the ROC analysis.

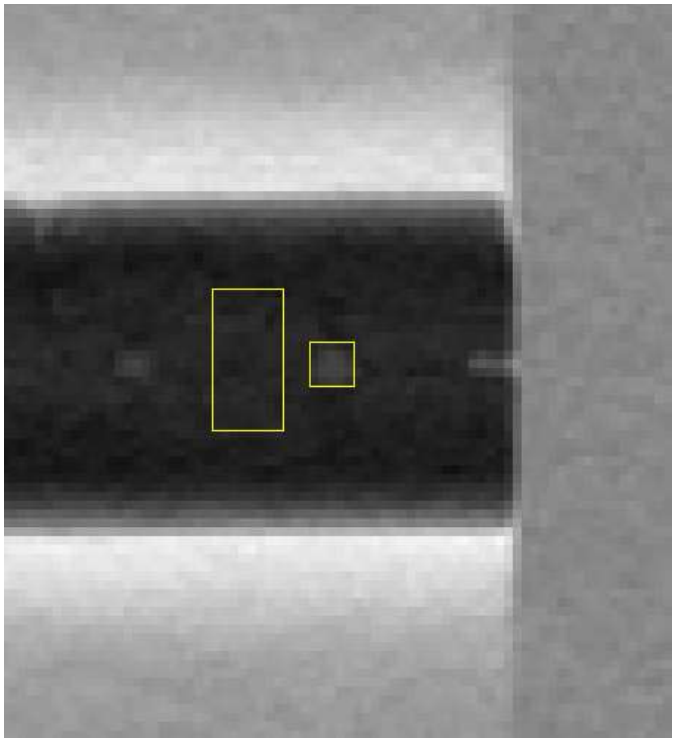

Fig 4 ROI setting for calculation of SNR and contrast.

A square lesion ROI (5 × 5 pixels) for simulating bone erosion and a rectangular ROI (16 × 8 pixels) for background.

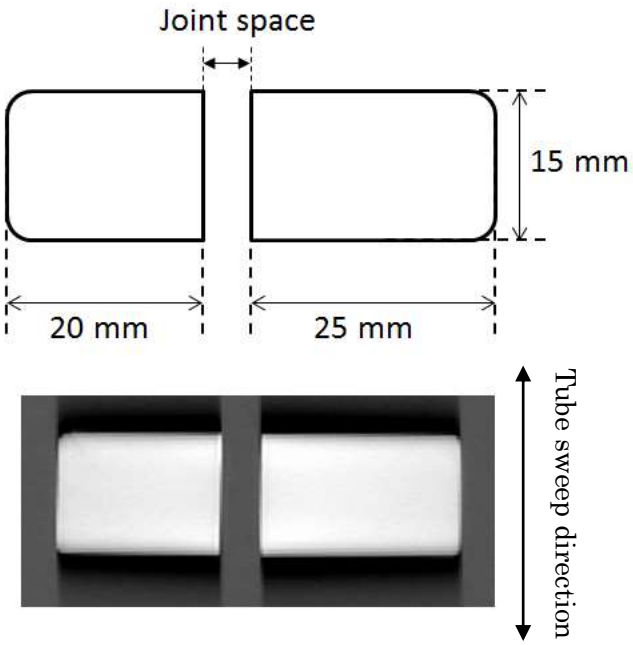

Fig 5 Image with illustration of joint space phantom.

The image with illustration shows an example of joint space widths of 5.0 mm made with use of 2 cylindrical TMA phantoms.

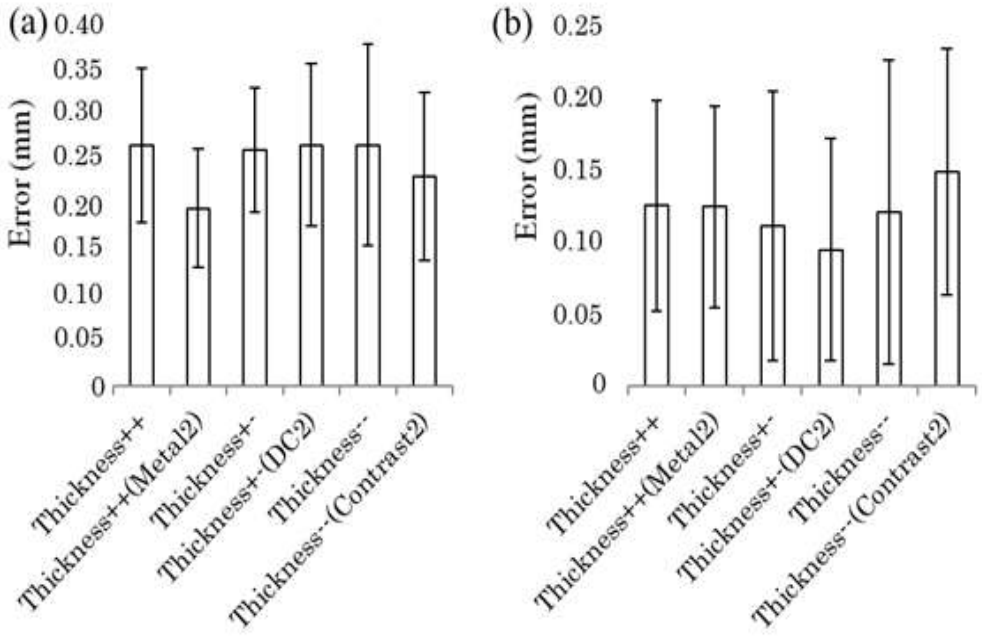

Fig 6 Comparison between accuracy assessment for different reconstruction filters.

a. Comparison of errors in the measurement of bone erosion between different reconstruction filters. The measured values of bone erosions in CT image are used as the gold standard to calculate the errors in tomosynthesis images. b. Comparison of errors in the measurement of joint space between different reconstruction filters.

In both graphs, the difference between reconstruction filters was not significant.

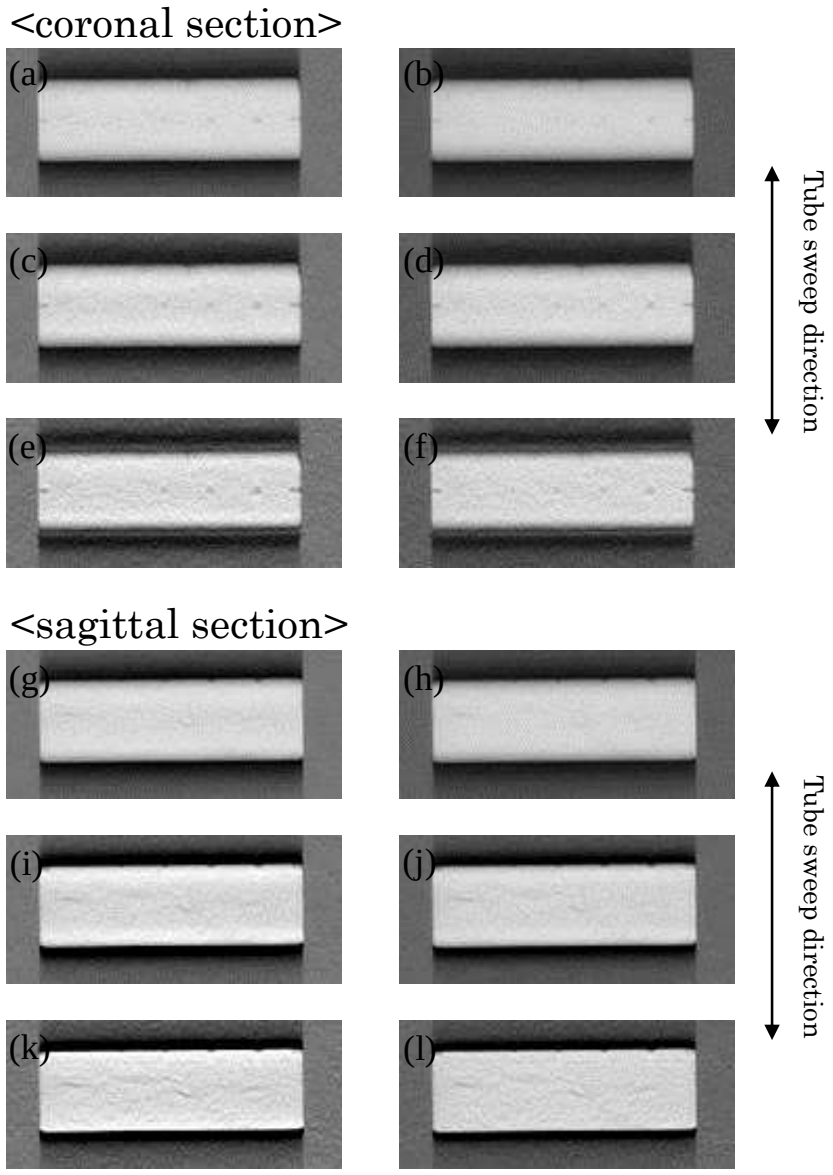

Fig 7 Bone erosion images for each reconstruction filter.

Coronal section: a. Thickness++ b. Thickness++(Metal2) c. Thickness+- d. Thickness+-(DC2) e. Thickness-- f. Thickness--(Contrast2)

Sagittal section: g. Thickness++ h. Thickness++(Metal2) i. Thickness+- j. Thickness+-(DC2) k. Thickness-- l. Thickness--(Contrast2).

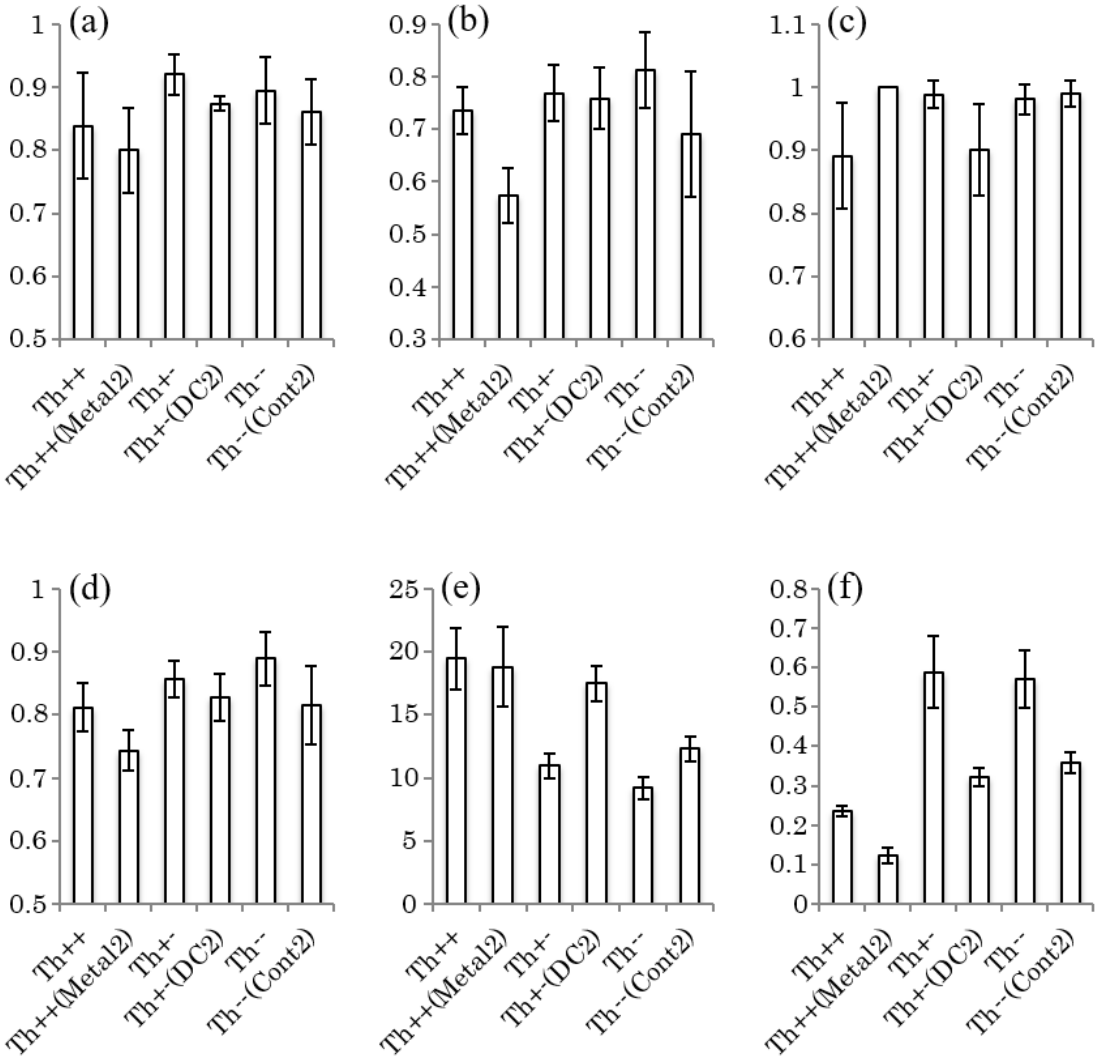

Fig 8 Results of each visibility assessment test: comparison of 6 reconstruction filters.

a. Az value b. sensitivity c. specificity d. accuracy e. SNR f. contrast.

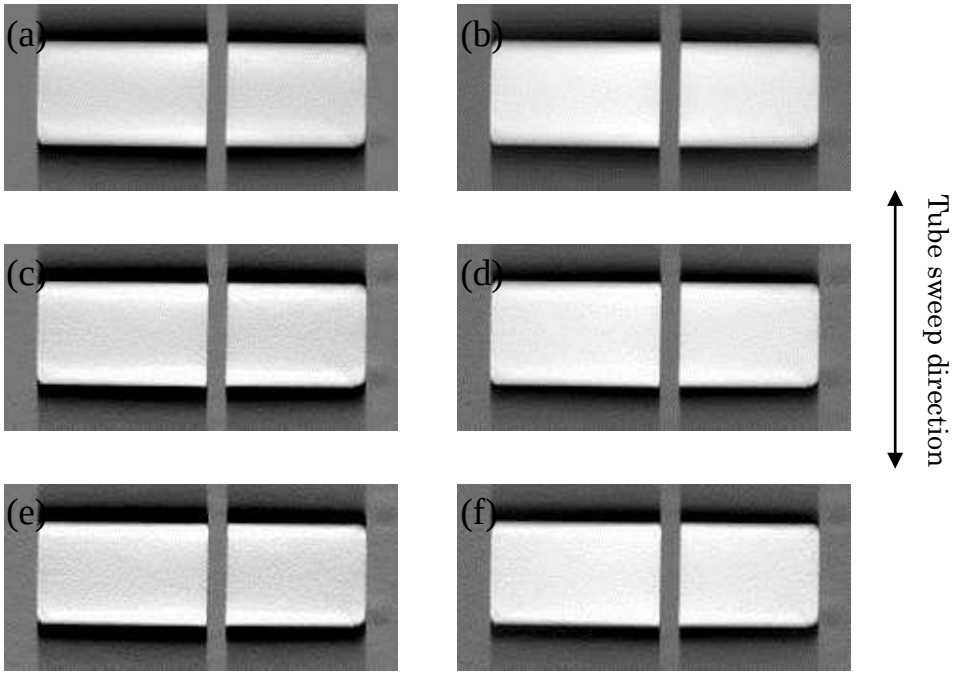

Fig 9 Joint space phantom images for each reconstruction filter (joint space width at 3.0 mm).

a. Thickness++ b. Thickness++(Metal2) c. Thickness+- d. Thickness+-(DC2) e. Thickness-- f. Thickness--(Contrast2).

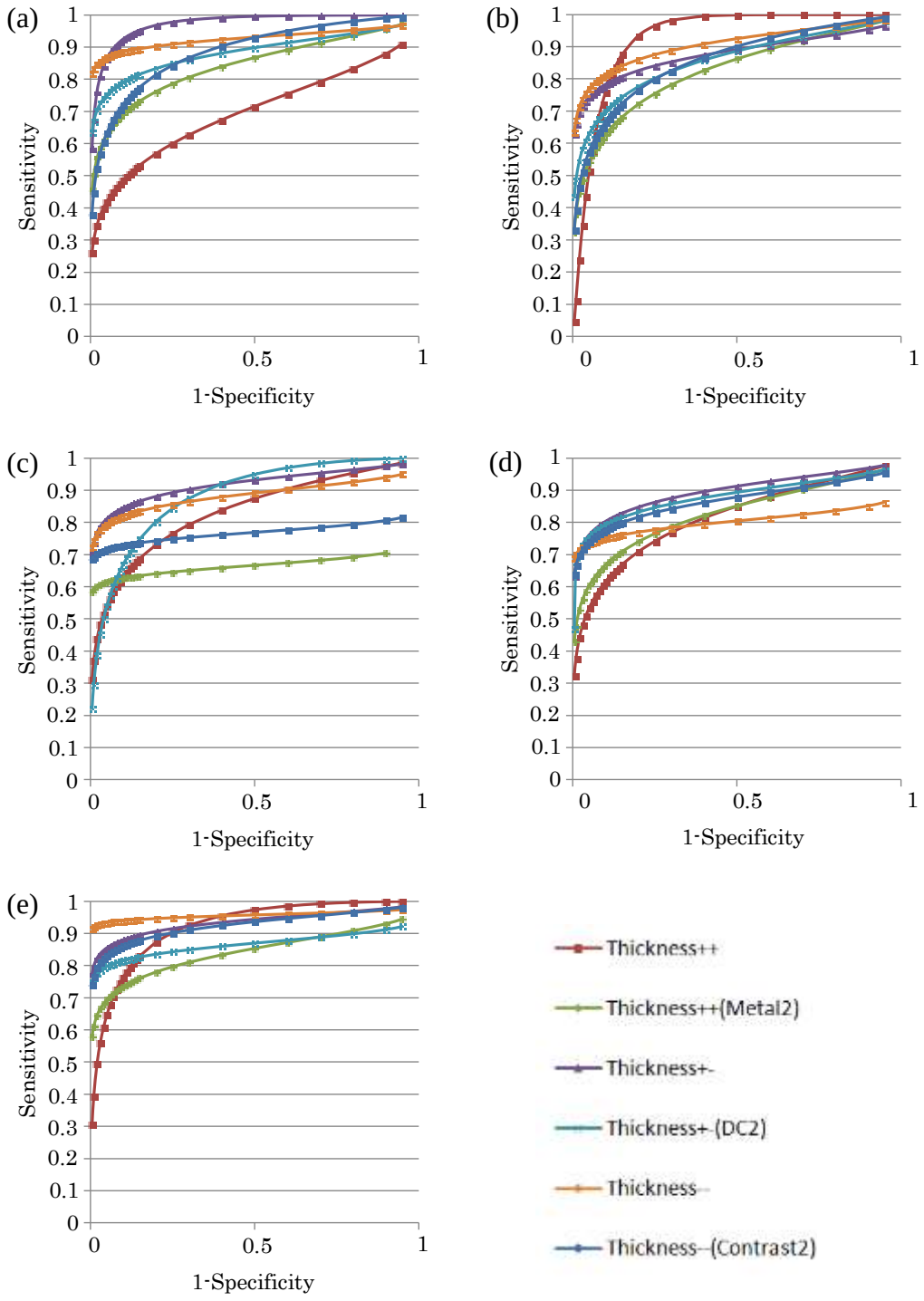

Fig S1 ROC curves of 5 readers.

(a) Reader A, (b) Reader B, (C) Reader C, (d) Reader D, (e) Reader E.

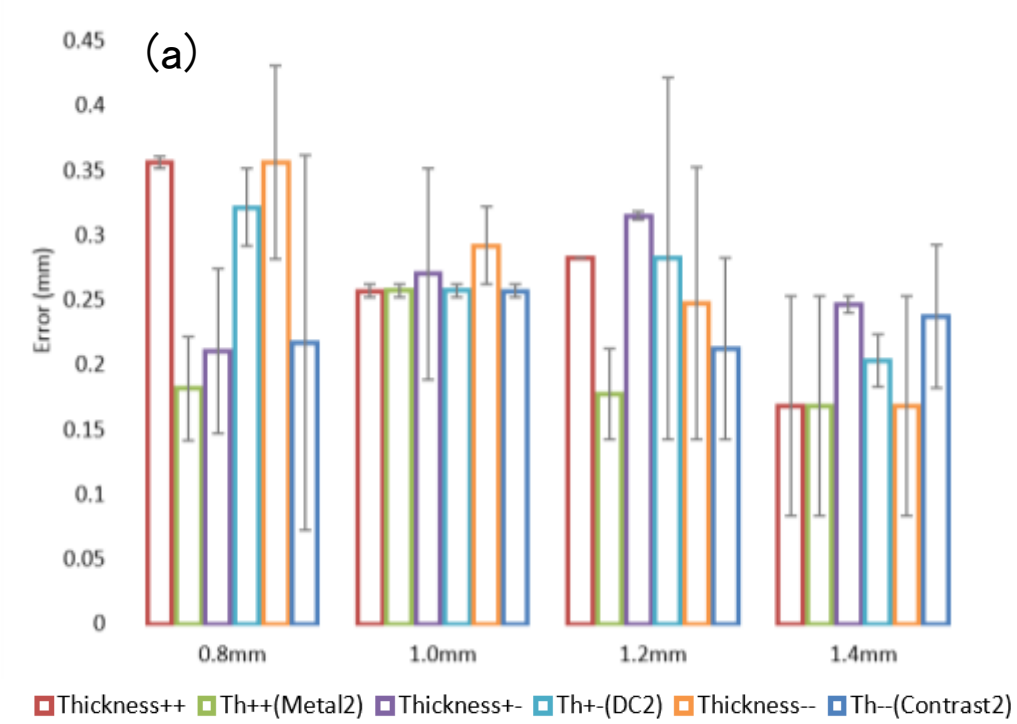

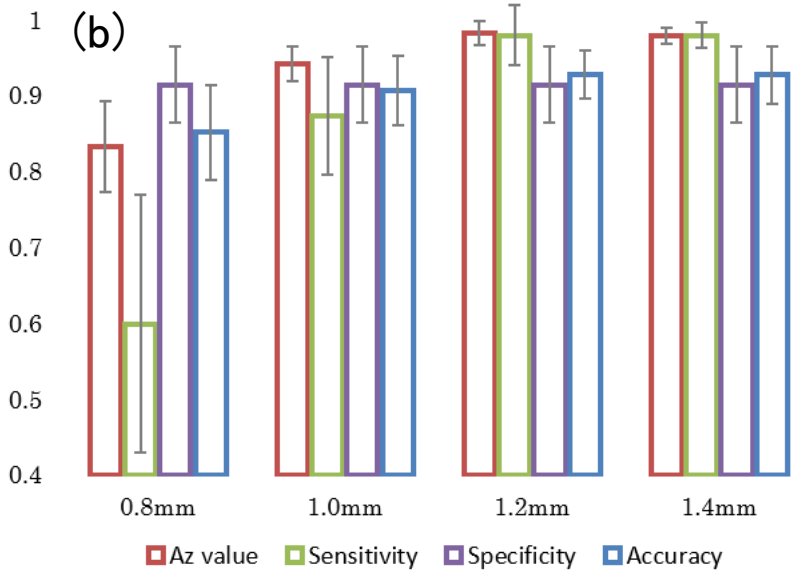

Fig S2 Error, Az value, sensitivity, specificity, and accuracy for each bone erosion size.

(a) Errors of simulating bone erosion size at each bone erosion size.

(b) Az value, sensitivity, specificity, and accuracy at each bone erosion size.

Table

Table 1 Imaging parameters of tomosynthesis.

			Bone erosion study	Joint space study
Imaging setting	Tube voltage (kV)		47	47
	Tube current (mA)		0.50	0.50
	Added filter		0.2mmCu+0.9mmAl	0.2mmCu+0.9mmAl
	FOV (inch)		9	9
	SID (mm)		1100	1100
	Frame rate (fps)		15	15
	Resolution		1028×1028 (High)	1028×1028 (High)
	Exposure time (s)		5.0	5.0
	Number of projections		74	74
	Sweep angle (°)		40	40
	Section Center height	(coronal)	110mm	21mm
		(sagittal)	105mm	
	Section range (mm)		30	36
	Reconstruction pitch (mm)		0.5	2.0
	Pixel size (μm)		300	300
	Effective dose (μSv)		11.47	11.47

Table S1 95% confidence interval of Az value in ROC analysis

	Reader A	Reader B	Reader C	Reader D	Reader E
Thickness++	0.5168-0.8387	0.8048-0.9806	0.6705-0.9329	0.6599-0.9169	0.7973-0.9760
Thickness++(Metal2)	0.6893-0.9349	0.6624-0.9269	0.4408-0.8434	0.6669-0.9271	0.4393-0.9843
Thickness+-	0.8819-0.9963	0.7241-0.9584	0.6808-0.9901	0.6592-0.9826	0.7398-0.9914
Thickness+-(DC2)	0.7267-0.9627	0.6950-0.9473	0.7346-0.9612	0.7222-0.9615	0.6376-0.9690
Thickness--	0.7823-0.9830	0.7631-0.9730	0.6489-0.9778	0.6020-0.9249	0.8012-0.9949
Thickness--(Contrast2)	0.7521-0.9592	0.7040-0.9454	0.5360-0.9151	0.6523-0.9669	0.7893-0.9811